

---

# A Simulation of Dynamic SPECT Using Radiopharmaceuticals with Rapid Clearance

Kenichi Nakajima, Noriyuki Shuke, Junichi Taki, Takashi Ichihara, Nobuatsu Motomura, Hisashi Bunko, and Kinichi Hisada

*Department of Nuclear Medicine, Kanazawa University Hospital, Kanazawa and Toshiba Nasu Works, Tochigi, Japan*

---

Data acquisition in SPECT assumes that there is no change in radionuclide distribution during data collection. However, this assumption is not valid in radiopharmaceuticals with rapid temporal changes in radioactivity. Artifacts and quantitative errors are studied using phantom studies, mathematical models, and clinical myocardial data. Projection data of each model were sequentially multiplied by weighting coefficients that varied mono-exponentially with time, and the SPECT images were reconstructed. A long data acquisition time in comparison to the clearance of the tracer can be a significant cause of artifact. When the myocardial septum-to-lateral count ratio is used as an index of distortion, a shorter acquisition time than the effective half-life of the tracer is required to reduce the error of the septum-to-lateral count ratio to within 10%. Since 180° rotation acquisition causes artifacts depending on the direction of rotation, 360° acquisition is preferable. Continuous repetitive rotation acquisition is a suitable method for dynamic SPECT to reduce quantitative errors and artifacts.

**J Nucl Med 1992; 33:1200-1206**

---

**S**ingle-photon emission computed tomography (SPECT) has become widely available in cardiac nuclear medicine and is now a standard modality for myocardial perfusion imaging (1-3). In particular, slight decreases in perfusion that may be overlooked on planar scintigraphy due to overlapping of radioactivity are often made clearer with SPECT. However, proper technique is more important in a SPECT study since inappropriate techniques produce significant artifacts both visually and quantitatively (4,5).

This study deals with the time-activity variation during SPECT data acquisition. Although SPECT data acquisition, in principle, needs no change in radioactivity over the imaging duration, this assumption is not valid in the case of radiopharmaceuticals with rapid kinetic changes (6-9). Among radiopharmaceuticals currently in use, this point is important for <sup>99m</sup>Tc-teboroxime, which has rapid clearance from the myocardium (10-13), and radioiodine-

labeled fatty acids, which undergo beta oxidation (14). However, only a few studies have evaluated the artifacts and quantitative errors seen in SPECT studies when rapidly changing radiopharmaceuticals are used (6-9). The threshold value of image acquisition time for clinical studies has not been fully investigated. To solve this problem, particularly in the field of cardiac SPECT study, we designed a simulation study with a myocardial phantom, mathematical model and clinical data for <sup>99m</sup>Tc-hexakis-methoxy-isobutyl-isonitrile (MIBI). This study evaluates:

1. Artifacts in dynamic SPECT.
2. The relationship between the effective half-life of the radiopharmaceutical and SPECT data acquisition time.
3. Comparison of 180° and 360° rotation acquisition.
4. The use of three-headed SPECT in comparison with a single-headed system.
5. The utility of continuous repetitive rotation acquisition with a tracer of rapid clearance.

## MATERIALS AND METHODS

### Procedures for Simulation and Assumption

Procedures used for the simulation of dynamic SPECT study were as follows: (1) projection images in 6° steps were generated. Thirty images for 180° rotation and 60 images for 360° rotation were made by either actual SPECT data acquisition or a mathematical model; (2) the projection images were modified by multiplying the coefficients, assuming monoexponential decay in radioactivity; (3) transaxial images were reconstructed by filtered backprojection with a ramp filter after preprocessing with a Butterworth filter; (4) attenuation correction was performed by the post-correction method proposed by Chang (15) in a cylindrical phantom (attenuation coefficient  $\mu = 0.11/\text{cm}$ ), however, no correction was performed in the myocardial phantom and clinical data; and (5) no correction for scatter was performed.

In this simulation, the following assumptions were made:

1. Clearance from the myocardium is uniform.
2. The structures around the heart show similarly uniform clearance.
3. The fraction of the absorption of radiation and Compton scatter are not affected by the amount of radiotracer in the body.
4. The statistical noise present in the projection image is similar even when the acquired count is low.

---

Received Sept. 27, 1991; revision accepted Dec. 4, 1991.

For reprints contact: Kenichi Nakajima, MD, Department of Nuclear Medicine, Kanazawa University Hospital, 13-1 Takara-machi, Kanazawa, 920 Japan.

In other words, this study did not evaluate the effect of noise, because we wanted to focus on the fundamental patterns of artifact and quantification in each myocardial segment.

**Simulation Models.** All SPECT data acquisitions were performed with a three-headed SPECT instrument (model GCA 9300A, Toshiba, Tokyo, Japan), which was equipped with high-resolution collimators (17). The full-width at half-maximum was 13 mm at the center of rotation with a radius of 20 cm, when the scinticameras were equipped with high-resolution collimators. Sixty  $128 \times 128$  matrix projection images were obtained with a  $6^\circ$  step mode. In all projection images with phantoms, the data acquisition time was determined so that for a high count image at least 250 cts/pixel was obtained.

The projection images were made using the following models:

- Model 1. A 20-ml syringe (19 mm in diameter), containing 80 MBq of [ $^{99m}\text{Tc}$ ]pertechnetate, that was placed in air.
- Model 2. A cylindrical phantom (132 mm in diameter) with uniform distribution of the radionuclide as a flood source. The water contained  $^{99m}\text{Tc}$  in a concentration of 0.07 MBq/ml.
- Model 3. A cylindrical phantom with 10 hot inserts. Each hot insert was a test tube (11 mm in diameter) containing [ $^{99m}\text{Tc}$ ]pertechnetate (1.8 MBq/ml), which was surrounded by water.
- Model 4. An anatomically realistic acrylic myocardial phantom (model RH2, Kyoto Kagaku, Kyoto), which was located in the body phantom (30 cm  $\times$  20 cm elliptical torso). The myocardial wall was filled with  $^{99m}\text{Tc}$  (0.7 MBq/ml), and the right and left ventricular chambers and mediastinum were filled with water. The lung was composed of wood powder.
- Model 5. Clinical data with  $^{99m}\text{Tc}$ -MIBI. Technetium-99m-MIBI (740 MBq) was injected in to two patients, and the projection data were acquired 90 min later. The scintigrams showed no perfusion abnormality in either patient. Each projection image was obtained 30 sec per view with a  $128 \times 128$  matrix and  $6^\circ$  step mode.
- Model 6. A mathematical model with heart and liver that simulated the  $^{99m}\text{Tc}$ -teboroxime study. Because the heart and liver show a decrease and increase in activity with time, respectively, the dynamic phantom model was difficult to make. Hence, we generated mathematically simulated projection images in this simulation. The contours of body, heart and liver were determined by a transaxial slice of  $^{99m}\text{Tc}$ -teboroxime study that was obtained with 3 to 6 min acquisition. In using these regions of interest (ROIS), we assumed that the radionuclide was distributed homogeneously in each region. During the rotation of the scinticamera, the myocardial count was assumed to decrease monoexponentially, while the hepatic count increased gradually as described below. A set of 60 projection profiles with  $6^\circ$  steps was made. Neither attenuation nor scatter were considered. Projection data with  $360^\circ$  and  $180^\circ$  rotations with clockwise and counterclockwise rotations were created.

In models 1 and 2, only  $360^\circ$  projection images were used. In model 3, both  $360^\circ$  and  $180^\circ$  data were produced. The  $180^\circ$  rotation data were generated by discarding the  $180^\circ$  arc data from

$360^\circ$  rotation data. Thus, the total count in  $180^\circ$  data had about a half of that in  $360^\circ$  data. In models 4 and 5,  $180^\circ$  rotation data were similarly generated, starting from the right anterior oblique  $42^\circ$  and rotating anteriorly to the left posterior oblique, as well as  $360^\circ$  rotation data. This rotation was defined as clockwise (CW) rotation. Similarly, counterclockwise (CCW)  $180^\circ$  rotation data from the left posterior oblique to right anterior oblique were produced.

**Temporal Change of Projection Images.** Each projection image was multiplied by a weighting coefficient that decayed sequentially with time. Monoexponential functions were used for the weighting values. No waiting time between stepped rotation projections was assumed. In models 1 to 5, the ratio of total acquisition time to the tracer's effective half-life was (percentage of remaining activity at the end of acquisition to the initial count is shown in brackets): 0 [100%], 1/12 [94%], 1/4 [84%], 1/2 [71%], 1 [50%], 2 [25%], and 3 [13%]. In model 6, parameters that were nearly equivalent to those of the  $^{99m}\text{Tc}$ -teboroxime study were utilized. The clearance from the myocardium was assumed to have an effective half-life of 7 min (monoexponential), while the liver showed increased radioactivity with a doubling time of 4.5 min and reached a plateau after 10 min. Since the essential pattern of artifact and quantitative analysis was performed in models 1 to 5, we studied only a typical example in this model in order to determine the effect of the coexistence of two organs having different types of time-activity variation.

**Three-Detector Model.** The use of a three-headed SPECT system was also examined by this approach to compare its results with a single-headed system. As in the clinical situation, each camera was assumed to rotate  $120^\circ$  in a counterclockwise direction (13). Since acquisition time was set to be the same as that of a single-headed camera, the total count was three times that for the three-headed system. However, the difference in count does not essentially affect the artifact patterns, although it affects the magnitude of statistical noise.

**Model for Continuous Repetitive Rotation Acquisition.** By assuming continuous alternate rotation of  $120^\circ$  using three-headed SPECT, which has been performed in  $^{99m}\text{Tc}$ -teboroxime studies (13), the relationship between the number of rotations during acquisition and the artifacts was investigated. The projection images were created by assuming 1, 2, 3, 4, 5, 10 and 15 rotations by the end of image acquisition.

## Data Analysis

First, decreases in regional counts and distortion of the images were visually evaluated. Circumferential profile analysis (18) was then applied to the transaxial image at the mid-portion of heart. The uptake of segments was analyzed with 60 segments in profile curves. Since artifacts were demonstrated as decreased activity in the septum and lateral walls, which became more evident with the longer acquisition time compared to the tracer's half-life, the ROIs were drawn over the septum and lateral walls. The septum-to-lateral ratio was calculated as an index of quantitative error using the count in these regions.

## RESULTS

### Phantom Models 1 to 3

Figure 1 shows the reconstructed transaxial image when the acquisition time is equal to the effective half-life. In the SPECT image of the syringe, the basic artifact pattern caused by variation of the time-activity curve was ob-

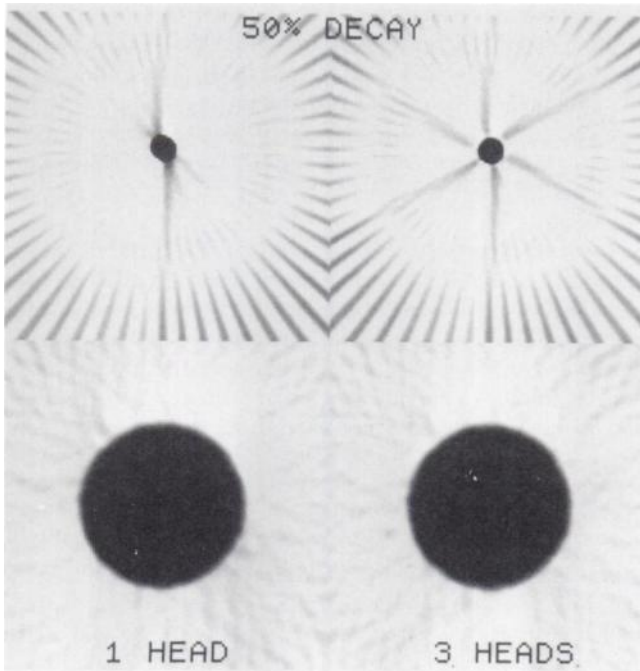


**FIGURE 1.** Syringe and cylindrical phantom assumed to be obtained with single-headed and three-headed cameras. The acquisition time was set to be the same as the tracer's effective half-life, that is, the percentage of count decay at the end of acquisition was 50%.

served. Namely, the artifact had tailings in two opposite directions. In three-headed SPECT, although the artifact was relatively suppressed, the reconstructed image had six tailings radially (Fig. 1, upper). A similar artifact was observed in the cylindrical phantom. However, no significant asymmetry of count distribution was recognized. Similar to the syringe model, triple-headed SPECT showed less artifacts around the edges than single-headed SPECT (Fig. 1, lower). The longer the acquisition time in comparison to the half-life of the tracer, the more significant was the resulting artifact. In the cylindrical phantom model with 10 hot inserts, the reconstructed image significantly differed between the 180° and 360° acquisition methods (Fig. 2). In this model, 180° acquisition was assumed to be performed in the upper half arc originating from the right horizontal direction (tubes 2–6 in the figure). The counts in the lower half hot inserts were underestimated, and the distortion of the shape of the tube was evident, particularly in the peripheral portion of the phantom. On the other hand, 360° acquisition showed no significant distortion in shape, although the counts in the tubes in the lower half was decreased. The difference in counts, depending on their location, was smaller in 360° acquisitions than in 180° acquisitions.

#### Myocardial Models 4 and 5

Figure 3 is a transaxial image of the myocardial phantom. Although no significant artifact was found visually, a difference in the septal and lateral counts was recognized in circumferential analysis. Hence, the septum-to-lateral

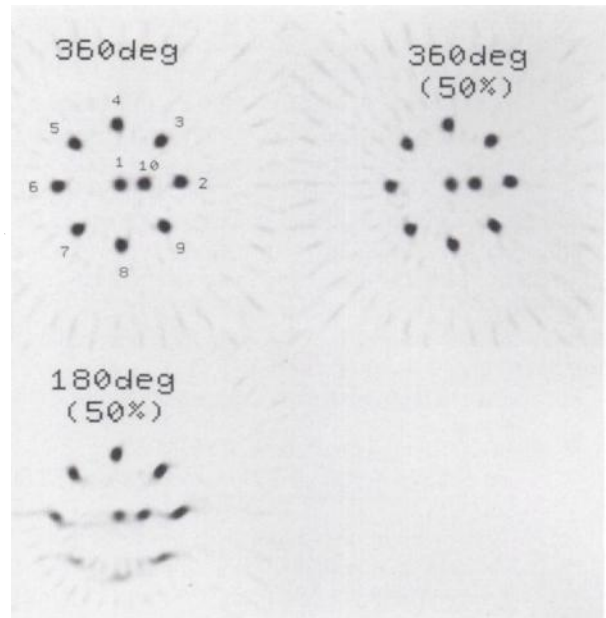


**FIGURE 2.** Cylindrical phantom model with ten hot inserts (left upper) original 360° acquisition, (right upper) 360° acquisition with 50% count decay, and (left lower) 180° acquisition with 50% count decay. Although maximum counts are normalized to 100% for display, the actual count of tube no. 3 in each image measured with circular ROIs was 10,892 counts, 8156 counts and 6256 counts, respectively. The counts of tube no. 7 were 10,348 counts, 7256 counts and 2540 counts, respectively.

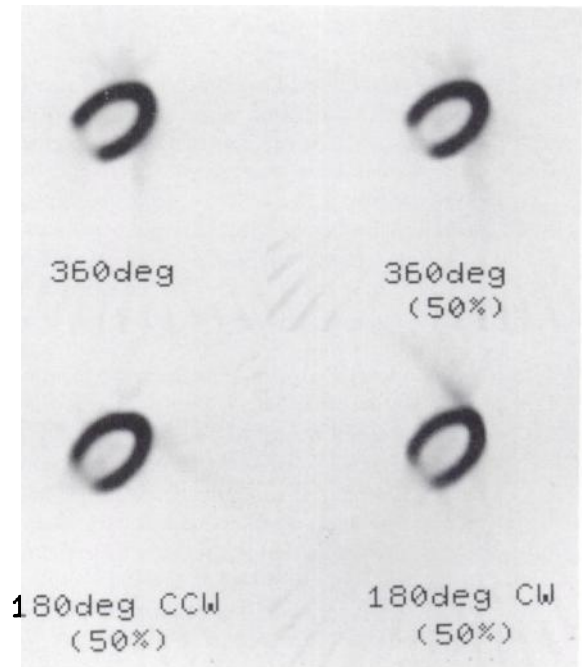


**FIGURE 3.** Myocardial phantom model. Original 360° acquisition image is in the left upper panel. When the acquisition time is equal to the effective half-life (50% count decay), 360° acquisition (right upper), 180° clockwise (right lower), and 180° counterclockwise (left lower) acquisitions are compared.

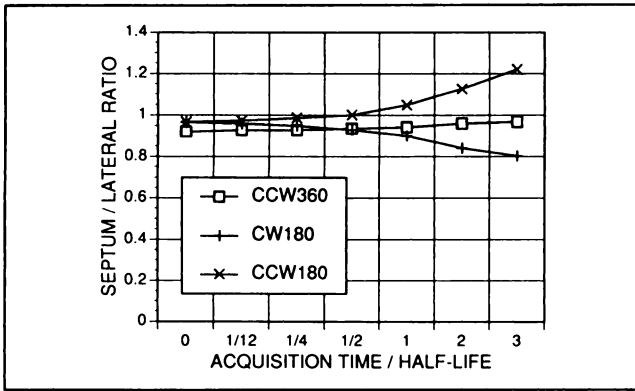


**FIGURE 4.** Relationship between septum-to-lateral count ratio and acquisition time-to-half-life ratio in the myocardial phantom model.

count ratio was calculated as a function of acquisition time (Fig. 4). When the scinticamera was rotated 180° in a clockwise direction, the septum-to-lateral ratio became smaller as the acquisition time increased, whereas in a counterclockwise rotation, the ratio became higher. In 360° acquisition, the septum-to-lateral ratio was relatively constant, irrespective of count decay during acquisition. Similarly, Figure 5 is the circumferential profile analysis performed on clinical data of the <sup>99m</sup>Tc-MIBI myocardium. In a 360° acquisition, the profile curve was essentially the same, even when the acquisition time was equal to the effective half-life. However, deviation of the profile curves from the theoretical value was observed in 180° acquisition. The relationship of the septum-to-lateral ratio to the acquisition time was similar to the phantom study (Fig. 6). From the data in Figures 4 and 6, it was postulated that the acquisition time should be less than half of the tracer's half-life to keep septum-to-lateral ratio errors to within 5%. To keep errors within 10%, the acquisition time should be less than the half-life of the tracer.

#### Mathematical Model 6

Figure 7 is the simulation result for the mathematical model, which includes heart and liver, with 180° rotation acquisition. Since the counts increased in the liver and

decreased in the heart with time, the direction of the tailing artifact was opposite. Although reconstruction was performed by assuming a slightly longer acquisition time (10 min) than the effective half-life of the tracer (7 min), the decrease in counts in the septal and lateral walls showed patterns similar to that seen in models 5 and 6. The presence of the liver did not influence the basic pattern of the artifact.

#### Continuous Repetitive Rotation Acquisition

The results for continuous repetitive acquisition with a three-headed system are shown in Figure 8. No noticeable artifact was visible on the reconstructed image. The use of a three-headed SPECT system, resulted in a septum-to-lateral ratio error that was relatively small, even in the single-rotation mode. The septum-to-lateral count ratio error was only approximately 5% when the acquisition time was three times the tracer's half-life. As the number of rotations increased during acquisition, the error became smaller and the septum-to-lateral ratio approached the theoretical value. From a quantitative point of view, more than two rotations appeared to be sufficient.

#### DISCUSSION

Reconstruction of tomographic images is performed by assuming that there is no temporal variation of count distribution. However, significant changes in radioactivity in some organs can be a cause of artifact or affect quantitative accuracy. This point has become an important issue because SPECT has become a routine procedure in cardiac nuclear medicine (2,3), and various radiopharmaceuticals with rapid kinetic changes have been developed (10-14). Moreover, the solution to this problem is becoming feasible as more high-sensitivity SPECT systems are developed (16,17). Bok et al. reported changes in resolution and distortion with time-activity variations (8). However, their study was performed qualitatively, and no quantitative approach or clinical threshold for acquisition time has been determined for myocardial SPECT. Hence, we designed this simulation study to clarify the characteristics of artifact and quantitative error in dynamic myocardial SPECT.

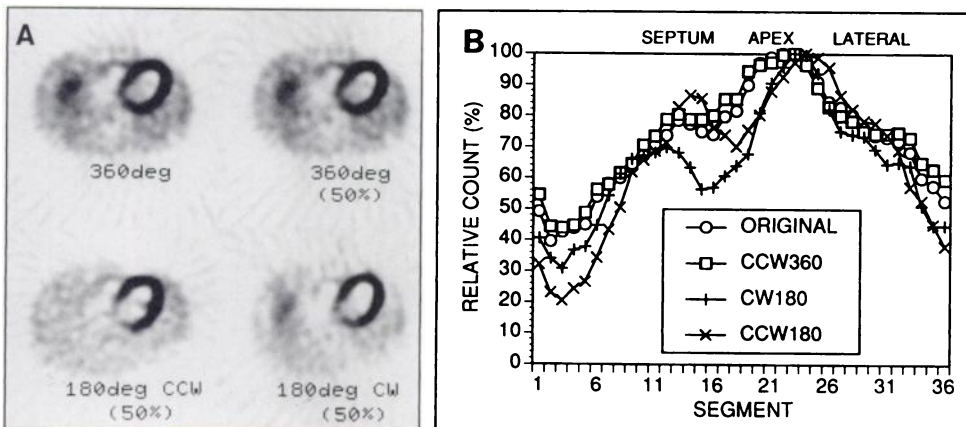


**FIGURE 5.** Technetium-99m MIBI myocardial model (A). Arrangement of the images is the same as in Figure 3. (B) The circumferential profiles in these transaxial images.

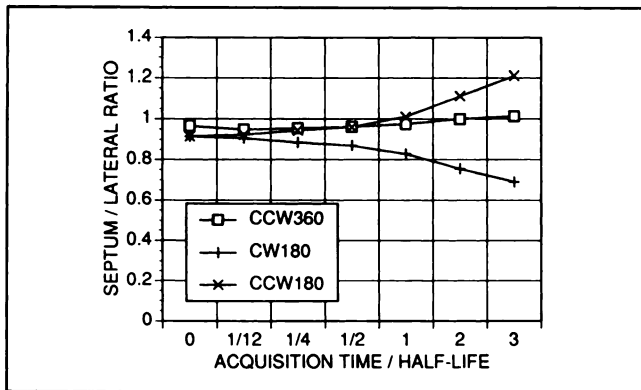


**FIGURE 6.** Relationship between septum-to-lateral count ratio and acquisition time-to-half-life ratio in the  $^{99m}\text{Tc}$ -MIBI myocardial model.

### Simulation Assumptions

A phantom model in which radioactivity distributes in a manner similar to that found in clinical conditions and gradually changes with time would be complex and difficult to generate. For a more practical approach, we investigated several simulations: from a simple syringe model to a more realistic myocardial model, for which several assumptions had been made.

The first assumption was that the clearance from the myocardium was uniform. This is not true in a pathologic myocardium. However, we accepted it because the fundamental artifact pattern would be more easily recognized with this simplification. The activity in the surrounding structures was also assumed to have the same clearance rate. This was valid in models 1 to 4, because there was no background activity around the myocardium. Actually, in a clinical setting, the background shows different temporal changes. However, the combination of the clearance rates in the target organ and background would vary significantly, and strict simulation of this condition was technically difficult. Nevertheless, the myocardial phantom model and the clinical  $^{99m}\text{Tc}$ -MIBI myocardium model showed essentially the same tendency in the circumferential profile analysis and the septum-to-lateral ratio. Even when the mathematical model with the liver was

analyzed, the basic pattern of artifact was the same as that postulated by models 1 to 6. As regards the third assumption, absorption of radiation and fraction of scatter were considered to be independent of the radioactivity, although the image quality was affected by the statistics of total acquired count. We used attenuation correction only in the cylindrical phantom that was filled with water, but this was not done in the clinical situations, because no satisfactory correction method for nonuniform attenuation tissue was available. For the fourth assumption, statistical noise in the high and low count images differs in practice. However, because the noise would not affect the quantitative relationship of the mean count in each myocardial segment, we did not modify or add to the statistical noise, although the signal-to-noise ratio in the reconstructed image would be influenced. Since we did not assume any time loss between each rotation projection, this condition applies only to the continuous rotation mode. The longer time loss between the stepped rotation projection will increase the total acquisition time, resulting in additional artifacts. However, if the total acquisition time is the same, i.e., actual acquisition time is reduced by eliminating the time for stepped rotation, the results are essentially identical in our simulation. Thus, although this simulation has limitations due to several assumptions, it would be a practical approach to investigate the fundamental artifacts and quantification in SPECT with dynamic temporal changes of the tracers.

### Improvements for Quantitative Accuracy

The results of this study suggest several methods for preventing artifacts.

*1. Short-Time Acquisition.* When the acquisition time is short enough compared with the effective half-life of the radiopharmaceutical, the artifacts will be negligible. For example, in a  $^{201}\text{Tl}$  myocardial SPECT study, suppose the effective half-life is about 4 hr and the acquisition time is 20 min, the ratio is then  $20/240 = 1/12$  (the second condition in this study), with no artifacts due to count decay seen in routine  $^{201}\text{Tl}$  studies. Recently developed three-headed SPECT has made possible short-time acquisition due to its capability for high sensitivity acquisition

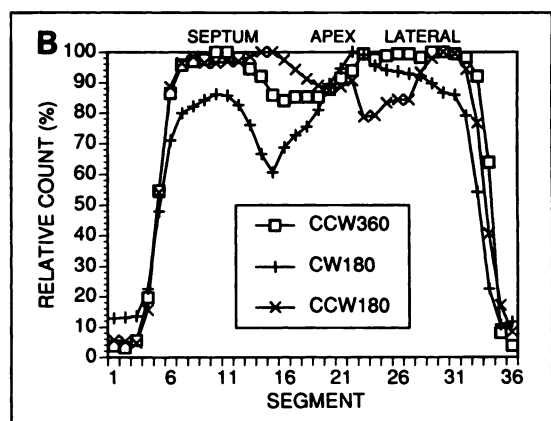
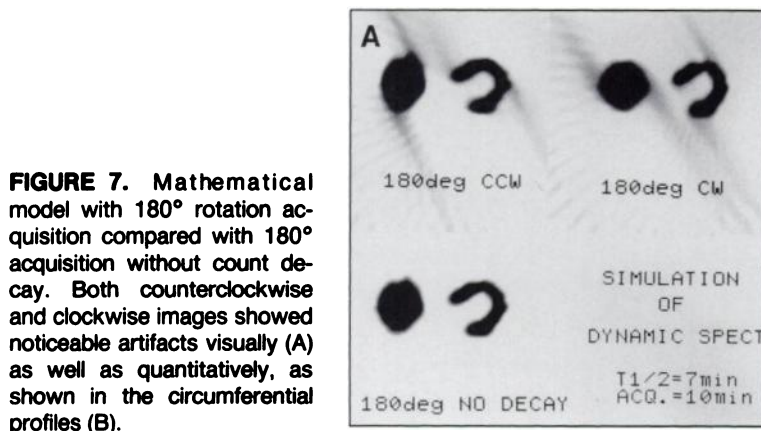


**FIGURE 7.** Mathematical model with  $180^\circ$  rotation acquisition compared with  $180^\circ$  acquisition without count decay. Both counterclockwise and clockwise images showed noticeable artifacts visually (A) as well as quantitatively, as shown in the circumferential profiles (B).

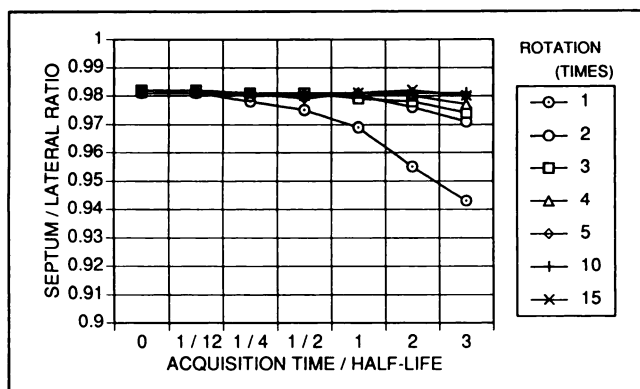


**FIGURE 8.** Relationship between the septum-to-lateral ratio and the number of rotations during acquisition.

(13,16,17). Multi-headed SPECT is suitable for dynamic studies in short-time intervals.

2. *360° Versus 180° Acquisition.* The difference in artifacts found in the 180° and 360° acquisition methods was more significant than we had expected. In single-headed SPECT, 180° rotation has been used to reduce acquisition time and improve image contrast, although some objections have been raised (19–22). However, from the viewpoint of image distortion and quantitative aspects, 360° acquisition seems to be preferable, because it provides complete backprojection from all directions. This is particularly important in the use of radiopharmaceuticals that show rapid dynamic changes.

3. *Multiple-Detector SPECT.* The three-headed SPECT acquisition simulated in this study was effective not only in reducing visual artifacts but also in improving quantitative accuracy as well. A three-headed system is advantageous because of its sensitivity and because the three cameras are in different positions simultaneously. Thus, even if the total acquisition count is the same, the radionuclide decay in a three-headed system can be reduced to one-third that in a single-headed system. Moreover, reducing the acquisition time in three-headed systems to one-third of that in single-headed systems can still contribute to the reduction of statistical noise with less artifacts.

4. *Continuous Repetitive Rotation Acquisition.* The clinical usefulness of continuous repetitive acquisition has been demonstrated in a  $^{99m}\text{Tc}$ -teboroxime study (13). In that study, since continuous alternate rotation seemed to improve quantitative accuracy by only two rotations per study, it should be applied in dynamic acquisition studies. If the quality of three scinticameras is well controlled and the cameras are in good balance, then a 120° rotation is sufficient and multiple alternate rotation will be a practical approach. Step-and-shoot repetitive rotation may be used as well. However, since one of the major purposes of repetitive alternate acquisition is reduction of data acquisition time without count loss, we prefer the continuous rotation mode. Let us suppose that a 5-sec interval is required between each stepped rotation projection. To

obtain 20 projections (60 projections per 360° rotation for three-headed cameras), an additional time of 100 sec (5 sec  $\times$  20) is necessary for a rotation. The percentage of time lost between each step will be significantly increased with more rapid acquisition.

### Clinical Implications

Single-headed systems with 180° rotation are liable to be affected by short acquisition times as compared to 360° acquisition. Although significant artifacts such as defects will be easily recognized and rejected as inappropriate reconstructions, problems arise from minor degrees of quantitative artifacts that are not apparent, as seen in the septum-to-lateral count ratio. From a quantitative point of view, the acquisition time must be less than half of the tracer's effective half-life to keep errors within 5%. Also, the clinical threshold of the acquisition time must be less than the tracer's half-life to keep errors within 10%.

Short-time acquisition can be applied to  $^{99m}\text{Tc}$ -teboroxime studies and to  $^{123}\text{I}$ -labeled fatty acid with rapid clearance in nuclear cardiology. Apart from cardiac studies, the same principle can be applied to hepatic and renal studies, where some radionuclides rapidly concentrate and clear away from the organ. Moreover, further development of radiopharmaceuticals with rapid metabolic changes will require dynamic SPECT.

In this study, the advantage of multi-detector systems was evident. However, the items discussed above can be applied to single-headed SPECT as well. For a  $^{99m}\text{Tc}$ -teboroxime study performed with single-headed SPECT, it is important to recognize that the acquisition time of 10 min, even assuming the effective half-life is about 10 min, may be a cause of quantitative inaccuracy. The direction of rotation should also be considered in quantitative analysis. Even though there is no noticeable artifact on the image, caution is necessary in quantitative evaluations, such as circumferential profile analysis and polar display analysis (18,23). Thus, short-time acquisition, 360° rotation and continuous repetitive rotation acquisition should also be evaluated for a single-headed system to enhance the quantitative accuracy.

### CONCLUSION

When radiopharmaceuticals with rapid clearance are used, image distortion and false-positive defects may result from tomographic reconstruction. When the ratio of acquisition time-to-effective half-life is increased, the myocardial septum-to-lateral ratio is calculated lower in clockwise 180° rotation, and higher in counterclockwise 180° rotation. To reduce quantitative errors of the septum-to-lateral ratio to less than 5%, the acquisition time must be shorter than half of the tracer's half-life. To keep this error within 10%, the acquisition time must be less than the half-life. Since the most drastic quantitative inaccuracy was observed in 180° acquisition, 360° acquisition is recommended. Continuous repetitive acquisition by three-headed SPECT can provide the most accurate quantitative

data and, hence, is suitable for dynamic acquisition for tracers showing rapid time-activity variation.

## REFERENCES

- O'Rourke RO, Chatterjee K, Dodge HT, et al. Guidelines for clinical use of cardiac radionuclide imaging, December 1986. A report of the American college of cardiology/American heart association task force on assessment of cardiovascular procedures (subcommittee on nuclear imaging). *Circulation* 1986;74:1469A-1482A.
- Schelbert RS. Current status and prospects of new radionuclides and radiopharmaceuticals for cardiovascular nuclear medicine. *Semin Nucl Med* 1987;17:145-181.
- Cerqueira MD, Harp GD, Ritchie JL. Evaluation of myocardial perfusion and function by single-photon emission computed tomography. *Semin Nucl Med* 1987;3:200-213.
- Halama JR, Henkin RE. Single photon emission computed tomography (SPECT). In: Freeman LM, ed, *Freeman and Johnson's clinical radionuclide imaging*, third edition. Orlando, FL: Grune & Stratton, Inc.; 1986;1593-1596.
- English RJ, Brown SE. Quality control requirement. In: *SPECT. Single-photon emission computed tomography: a primer*. New York: The Society of Nuclear Medicine; 1986;25-46.
- Holden JE, Ip WR. Continuous time-dependence in computed tomography. *Med Phys* 1978;5:485-490.
- Ip WR, Holden JE, Winkler SS. A study of the image discrepancies due to object time dependence in transmission and emission tomography. *Phys Med Biol* 1983;28:952-953.
- Bok BD, Bice AN, Clausen M, Wong DF, Wagner HN. Artifacts in camera-based single-photon emission tomography due to time activity variation. *Eur J Nucl Med*; 1987;13:439-442.
- Maeda H, Takeda K, Matsumura K, et al. The influence of the time activity variation on dynamic SPECT images in camera-based SPECT. *Jpn J Nucl Med* 1991;28:27-34 (in Japanese).
- Narra RK, Nunn AD, Kuczynski BL, Feld T, Wedeking P, Eckelman WC. A neutral technetium-99m complex for myocardial imaging. *J Nucl Med* 1989;30:1830-1837.
- Seldin DW, Johnson LL, Blood DK, et al. Myocardial perfusion imaging with technetium-99m-SQ30,217: comparison with thallium-201 and coronary anatomy. *J Nucl Med* 1989;30:312-319.
- Stewart RE, Schwaiger M, Hutchins GD, et al. Myocardial clearance kinetics of technetium-99m-SQ30217: a marker of regional myocardial blood flow. *J Nucl Med* 1990;31:1183-1190.
- Nakajima K, Taki J, Bunko H, et al. Dynamic acquisition with a three-headed SPECT system: application to technetium 99m-SQ30217 myocardial imaging. *J Nucl Med* 1991;32:1273-1277.
- DeGrado TR, Holden JE, Ng CK, Raffel DM, Gatley SJ. Quantitative analysis of myocardial kinetics of 15-p-[iodine-125]iodophenylpentadecanoic acid. *J Nucl Med* 1989;30:1211-1218.
- Chang LT. A method for attenuation correction in radionuclide computed tomography. *IEEE Trans Nucl Sci* 1978;NS-25:638-643.
- Lim CB, Gottschalk S, Walker R, et al. Triangular SPECT system for 3-D total organ volume imaging. *IEEE Trans Nucl Sci* 1985;NS-32:741-747.
- Ichihara T, Matsudaira M, Yamada M. Basic development of the Toshiba digital gammacamera, model GCA-9300A. In: Hisada K, ed. *An atlas of second generation SPECT*. Tokyo: Maruzen Co. Ltd.; 1991;13-19.
- Burrow RD, Pond M, Schafer AW, et al. Circumferential profiles: a new method for computer analysis of thallium-201 myocardial perfusion images. *J Nucl Med* 1979;20:771-777.
- Tamaki N, Mukai T, Ishii Y, et al. Comparative study of thallium emission myocardial tomography with 180° and 360° data collection. *J Nucl Med* 1982;23:661-666.
- Coleman RE, Jaszczak RJ, Cobb FR. Comparison of 180 and 360 data collection in thallium-201 imaging using single-photon emission computed tomography (SPECT): concise communication. *J Nucl Med* 1982;23:655-660.
- Go RT, MacIntyre WJ, Houser TS. Clinical evaluation of 360° and 180° data sampling techniques for transaxial SPECT thallium-201 myocardial perfusion imaging. *J Nucl Med* 1985;26:695-706.
- Eisner RL, Nowak DJ, Pettigrew R, Fajman W. Fundamentals of 180° acquisition and reconstruction in SPECT imaging. *J Nucl Med* 1986;27:1717-1728.
- Garcia EV, Van Train K, Maddahi J, et al. Quantification of rotational thallium-201 myocardial tomography. *J Nucl Med* 1985;26:17-26.

## EDITORIAL

# SPECT of Rapidly Cleared Tracers: Imaging a Cheshire Cat

"I wish you wouldn't keep appearing and vanishing so suddenly. You make one quite giddy."

Lewis Carroll, *Alice in Wonderland*

Things were easier in the old days. Tracers stayed in place long enough to get decent pictures with a scanner that crawled from one pixel to the next in a plodding but somehow confidence inspiring manner. The modern age has come, and with it a multitude of new tracers with biological and physical half-lives measured in minutes rather than hours.

A fundamental principle of single-photon emission computed tomography (SPECT) is that the object(s) being studied remain constant throughout the acquisition. Activity is assumed to be constant within the structure and the position of structures is constant relative to one another. Each projection includes the entire object being studied and all projections view the same object, differing only in perspective angle. These assumptions are in fact occasionally violated. Washout and redistribution of <sup>201</sup>Tl has been documented to occur over a matter of minutes. Iodoamphetamine distribution within the brain changes significantly over a period of 1 hr. Despite this, clinically useful SPECT images of these tracers are routinely obtained with acquisition

times of 30-40 min. Other imaging situations are less tolerant. Bone SPECT of the hips is frequently contaminated by artifacts resulting from the filling of the bladder with tracer. Newer tracers possess rapid kinetics, rich with information about blood flow and physiology.

The recent approval of <sup>99m</sup>Tc-teborexime has offered the potential of rest/stress myocardial perfusion imaging in a matter of minutes; a boon to the throughput demands of modern economics. Radiolabeled fatty acids offer the potential of in-vivo assessment of myocardial metabolism without the cost and expense of a cyclotron and PET scanner. These tracers present a challenge to standard tomographic imaging. Until recently, it has been widely assumed that dy-

Received Jan. 14, 1992; accepted Jan. 16, 1992.

For reprints contact: Jack E. Juni, MD, Department of Nuclear Medicine, William Beaumont Hospital, 3601 West 13 Mile Road, Royal Oak, MI 48073-6769.